Available online at www.sciencedirect.com

SciVerse ScienceDirect

Ceramics International 39 (2013) 6481–6487

CERAMICS INTERNATIONAL

www.elsevier.com/locate/ceramint

Fabrication of all-solid-state battery using $Li_5La_3Ta_2O_{12}$ ceramic electrolyte

Masashi Kotobuki*, Kiyoshi Kanamura

Department of Applied Chemistry, Graduate School of Urban Environmental Science, Tokyo Metropolitan University, 1-1 Minami-Ohsawa, Hachioji, Tokyo 192-0397, Japan

Received 22 November 2012; received in revised form 22 January 2013; accepted 24 January 2013
Available online 31 January 2013

Abstract

The chemical and electrochemical properties of $Li_5La_3Ta_2O_{12}$ (LLTa) solid electrolyte were extensively investigated to determine its compatibility with an all-solid-state battery. A well-sintered LLTa pellet with a garnet-like structure was obtained after sintering at 1200 °C for 24 h. Li ion conductivity of the LLTa pellet was estimated to be 1.3×10^{-4} S cm^{-1}. The LLTa pellet was stable when in contact with lithium metal. This indicates that Li metal anode, which is the best anode material, can be applied with the LLTa system. A full cell composed of $LiCoO_2$/LLTa/Li configuration was constructed, and its electrochemical properties were tested. In the resulting cyclic voltammogram, a clear redox couple of $LiCoO_2$ was observed, implying that the all-solid-state battery with the Li metal anode was successfully operated at room temperature. The redox peaks of the battery were still observed even after one year of storage in an Ar-filled glove-box. It can be concluded that the LLTa electrolyte is a promising candidate for the all-solid-state battery because of its relatively high Li ion conductivity and good stability when in contact with Li metal anode and $LiCoO_2$ cathode.

Keywords: All-solid-state battery; Solid electrolyte; Lithium battery; Li metal anode

1. Introduction

Electrolytes for lithium-ion batteries generally contain flammable organic solvents that sometimes cause serious safety problems, such as electrolyte leakage and fire hazard [1]. An all-solid-state lithium battery, consisting of solid electrodes and non-flammable solid electrolyte, is expected to overcome these safety problems [2].

It is well known that high lithium ion conductivity, wide electrochemical window, and good chemical stability against electrode materials are required for the solid electrolytes [3]. The Li ion conductivity of ceramic electrolytes is generally lower than those of non-aqueous liquid electrolytes, but some oxides, such as $Li_{0.35}La_{0.55}TiO_3$ (LLT) [4–6] and $LiTi_2(PO_4)_3$ (LTP) [7,8], possess high Li conductivities at approximately 10^{-3}–10^{-4} S cm^{-1}. These oxides are acceptable for use in all-solid-state batteries because of their high transport number ($t \approx 1$) [9]. Therefore, many research groups have focused on these oxides in applications utilizing all-solid-state rechargeable lithium ion batteries. However, due to the easy reduction of Ti^{4+} to Ti^{3+} (2.1 V vs. Li/Li$^+$), anode materials are restricted in their application with LLT and LTP systems, which limits the energy and power densities of the all-solid-state rechargeable lithium ion batteries [10].

In the last several years, a series of garnet-like structural compounds have been investigated as a novel family of fast lithium ion conductors by Weppner et. al. [11–14]. Among them, $Li_5La_3Ta_2O_{12}$ (LLTa) and $Li_7La_3Zr_2O_{12}$ (LLZ) have generated much attention because of their stability in the presence of Li metal [11,14].

Li metal anode has the largest capacity of all anode materials due to a lack of matrix components, 3862 mA h g^{-1} [15], which is 10 times larger than that of the currently used graphite anode (372 mA h g^{-1} [16]). Therefore, the all-solid-state battery with Li metal anode is expected to meet the demand for development of power sources with higher energy and power densities. Recently, an application of the

*Corresponding author. Present address: Hakodate National College of Technology, Japan. Tel./fax: +81 138 59 6466.
E-mail addresses: kotobuki@hakodate-ct.ac.jp, ms943508@hotmail.de (M. Kotobuki).

0272-8842/$ - see front matter © 2013 Elsevier Ltd and Techna Group S.r.l. All rights reserved.
http://dx.doi.org/10.1016/j.ceramint.2013.01.079

LLZ electrolyte for all-solid-state battery has been studied [17,18]. However, no such study has been reported with the LLTa electrolyte.

In this study, we investigated in detail the chemical and electrochemical properties of LLTa and then attempted a fabrication of all-solid-state battery using the LLTa solid electrolyte.

2. Experimental

$Li_5La_3Ta_2O_{12}$ (LLTa) was prepared by a solid-state reaction. $LiNO_3$ (Kanto Kagaku, Japan), $La(OH)_3$ (Shinetsu kagaku, Japan) and Ta_2O_5 (Kanto Kagaku, Japan) were mixed using a planetary ball mill (Mono-mill P-6, Fritsch GmbH) in isopropanol (Wako chemical, Japan). After evaporation of the isopropanol at room temperature, the mixture was calcined at 700 °C for 12 h. The calcinated powder was formed into a pellet with a diameter of 13 mm and then sintered again at 1000–1200 °C for 24 h. After sintering, the pellets were polished to obtain a flat surface and to control a pellet thickness of 1 mm.

A cross section of the LLTa pellet was observed through scanning electron microscopy (SEM, JEOL). The crystal phases of the pellet were identified by X-ray diffraction (XRD, RINT-Ultima, Rigaku) using Cu Kα radiation.

The Li ion conductivity of the LLTa pellet was determined by the AC impedance method with a SI1260 impedance/gain-phase analyzer (Solartron analytical). Prior to measurement, Au was sputtered onto both sides of the pellet to ensure complete electrical contact. The data were collected with a voltage signal of ± 5 mV in a frequency range of 100 Hz–1 MHz.

Stability of the LLTa pellet against molten Li metal was tested through the contact of the pellet with molten Li on a Ni plate in Ar-filled glove-box. This contact was maintained for 72 h, and then the pellet was removed from the molten Li and then analyzed by XRD.

The electrochemical window of the LLTa pellet was measured by cyclic voltammetry (CV) using a cell with Li/LLTa/Au configuration (HSV-100, Hokuto Denko co.). The measurement was conducted at a scan rate of 10 mV min^{-1} with the potential range from -0.5 to 5.0 V vs. Li/Li^+ at room temperature.

A $LiCoO_2$ cathode was prepared on the LLTa pellet by the sol–gel method. A mixture of $LiCoO_2$ powder (Celceed 10N, Nippon Chemical Industrial Co. Ltd., Japan) and its precursor sol, composed of CH_3COOLi, $Co(CH_3COO)_2 \cdot 4H_2O$, *i*-$C_3H_7OH$, CH_3COOH, H_2O, and poly-vinylpyroridone (molar ratio = 1.1:1:20:10:70:1), was impregnated onto the LLTa pellet. The impregnated pellet was calcined at 700 °C for 2 h to obtain $LiCoO_2$/LLTa pellet [19]. The thickness of the cathode was approximately 10 μm (ca. 1 mg). The impregnated $LiCoO_2$ was characterized by XRD and Raman spectroscopy (NRS-1000, JASCO) with 532 nm laser radiation. In order to construct an all-solid-state battery with Li/LLTa/$LiCoO_2$ configuration, Li metal was put onto the LLTa side of the $LiCoO_2$/LLTa pellet. The CV measurement of the all-solid-state battery was performed at a scan rate of 1 mV min^{-1} with a scan range of 3.3–4.2 V vs. Li/Li^+ at room temperature.

3. Results

The LLTa pellet was sintered at various temperatures. Cross-sectional SEM images are displayed in Fig. 1. With the increase of calcination temperature, the pellets were sintered well. At 1100 °C sintering (Fig. 1(b)), many facets as well as a few interstices were observed. The interstices were minimally observed in the LLTa pellet sintered at 1200 °C (Fig. 1 (c)); however, many grain boundaries were

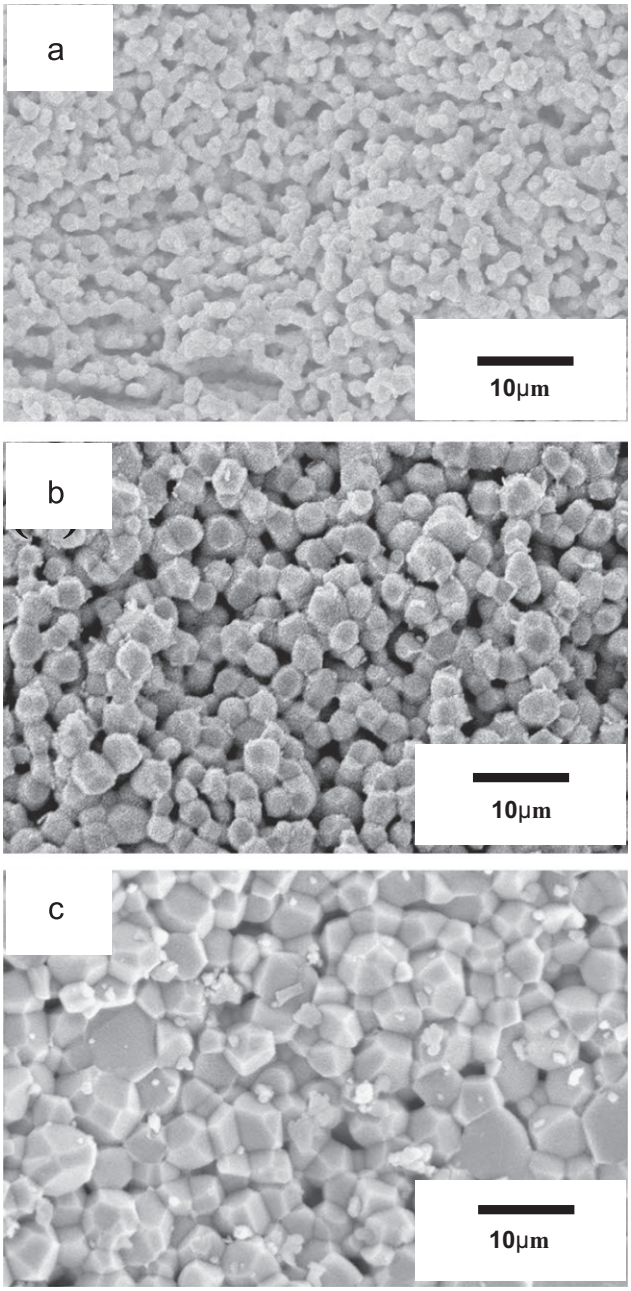

Fig. 1. Cross-sectional SEM images of LLTa pellet after sintering at (a) 1000 °C, (b) 1100 °C, and (c) 1200 °C for 24 h.

still observed. The estimated densities of the pellets sintered at 1000, 1100, and 1200 °C were 3.7, 4.3, and 5.7 g cm^{-3}, respectively, which correspond to 61%, 70%, and 93% of its theoretical density (6.1 g cm^{-3}).

The XRD patterns of LLTa pellets calcined at various temperatures are depicted in Fig. 2. All of the observed diffraction peaks were well-matched with the standard peaks of the LLTa with a garnet structure (PDF 45-0110), and no impurity phase was observed, indicating that LLTa pellets with a garnet-like structure were successfully prepared. These diffraction peaks became sharper with an increase in the calcination temperature.

A complex impedance plot of the LLTa pellet sintered at 1200 °C is revealed in Fig. 3. A semicircle and Warburg-type impedances were observed in the high and low frequency regions, respectively. The tail that was observed at low frequencies corresponds to a well-known behavior of ionically conductive ceramics [20]. A similar behavior has been observed in other garnet-like ceramic conductors [11,13,21–23]. The semicircle implied two kinds of resistance. One is the bulk resistance which means a resistance when Li ions move in the crystal grain. The other is the grain-boundary resistance. The grain-boundary resistance is a resistance when Li ions go beyond grain-boundaries. The total resistance is a sum of the bulk and the grain-boundary resistances. The bulk and total resistances can be estimated from intersections at the low and high frequency sides of the semicircle in the impedance spectrum (Fig. 3), respectively. Therefore, the bulk and total conductivities can be calculated by using the following equation.

$$\sigma = \frac{t}{RA}$$

In the equation, σ, t, R, and A mean conductivity (S/cm), thickness of electrolyte (cm), resistance (Ω), and electrode area (cm^2), respectively. The bulk (σ_{bulk}) and total (σ_{total}) conductivities were 3.9×10^{-4} and 1.3×10^{-4} S cm^{-1}, respectively.

In order to test the stability of the LLTa pellet in contact with Li metal, the LLTa pellet was placed in molten Li metal for 72 h. No visual change of the LLTa pellet was observed (Fig. 4). The XRD patterns of the LLTa pellet before and after contact were also completely identical, and new diffraction peaks did not appear (Fig. 5), indicating that the LLTa was stable when in contact with Li metal.

A cyclic voltammetry measurement (CV) of Li/LLTa/Au cell was conducted to determine the electrochemical window of the LLTa (Fig. 6). Peaks associated with the formation of Au–Li alloy as well as the extraction of the Li from the alloy were clearly observed, indicating that the lithium ion could be transferred through the LLTa electrolyte without any inferiority of LLTa. At the anodic potential side, the LLTa was stable up to 5 V.

An all-solid-state battery with Li metal anode and LLTa solid electrolyte was fabricated by using $LiCoO_2$ cathode. The $LiCoO_2$ cathode was approximately 10 μm thick on

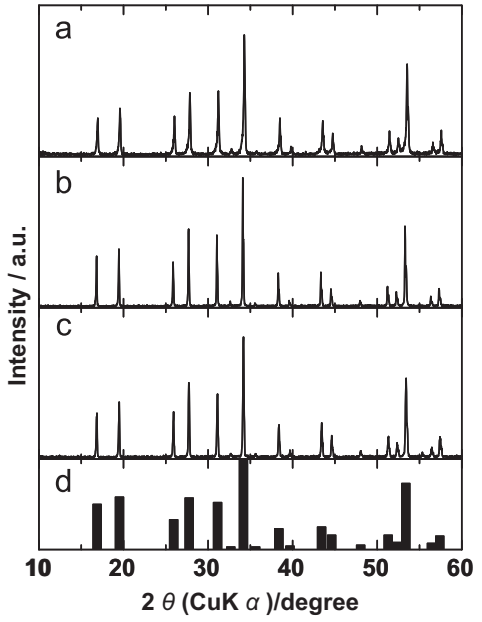

Fig. 2. XRD patterns of LLTa pellet after sintering at (a) 1000 °C, (b) 1100 °C, and (c)1200 °C for 24 h and (d) the standard pattern of LLTa (PDF 45-0110).

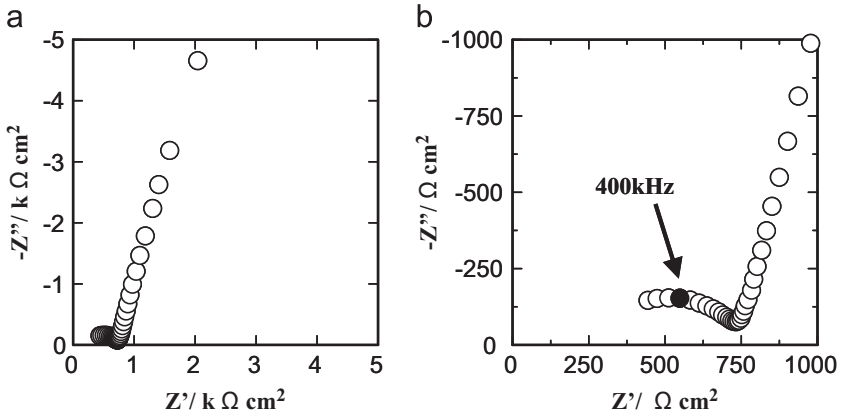

Fig. 3. Complex impedance plot of LLTa pellet sintering at 1200 °C for 24 h: (a) whole plot and (b) magnified plot around the origin.

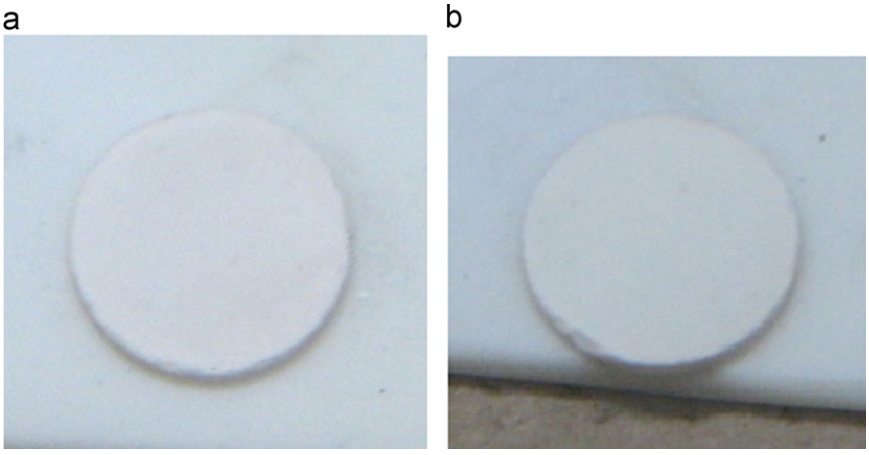

Fig. 4. Photos of LLTa pellet (a) before and (b) after contact with molten Li metal for 72 h.

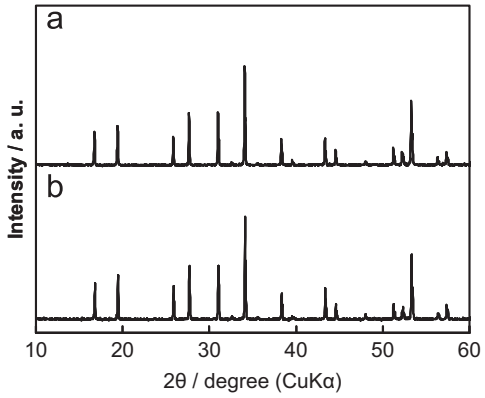

Fig. 5. XRD patterns of LLTa pellet (a) after and (b) before contact with molten Li metal for 72 h.

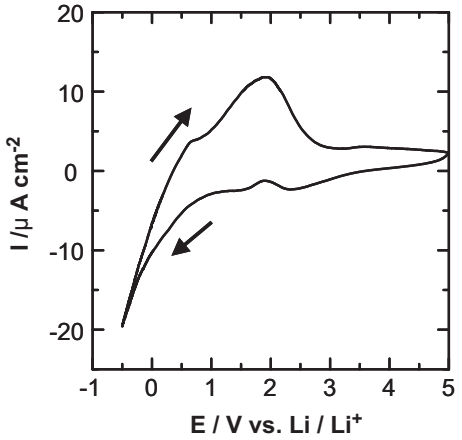

Fig. 6. Cyclic voltammogram of Li/LLTa/Au cell at a scan rate of 10 mV min^{-1} in the potential range from −0.5 to 5 V vs. Li/Li^+.

the LLTa and was prepared by the sol–gel method. The XRD patterns showed clear diffraction peaks of $LiCoO_2$ (Fig. 7). All other peaks were attributed to LLTa, and no impurity phase was detected. Clear bands in the Raman spectrum were confirmed at 483 and 594 cm^{-1} (Fig. 8).

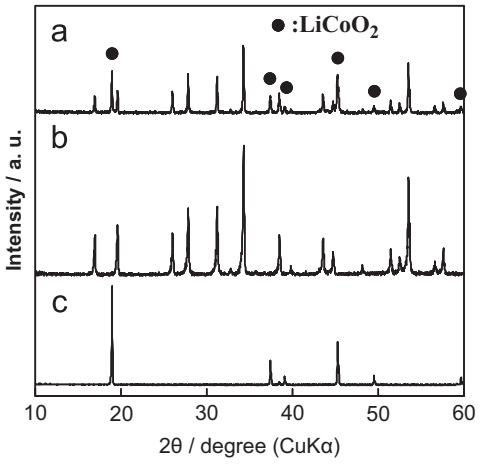

Fig. 7. XRD patterns of (a) LLTa pellet after $LiCoO_2$ impregnation, (b) as-prepared LLTa pellet and (c) $LiCoO_2$ powder.

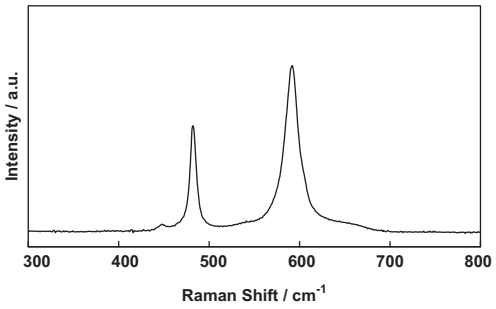

Fig. 8. Raman spectrum of LLTa pellet after $LiCoO_2$ impregnation.

These bands are attributed to the E_g and A_{1g} Raman active modes of high temperature (HT)-$LiCoO_2$ with a hexagonal layered structure [24], which is a favorable structure for the cathode of lithium battery [25]. A small Raman band at 450 cm^{-1} was also observed. This band is associated with the F_{2g} mode of low temperature (LT)-$LiCoO_2$ in the cubic spinel phase [26,27].

An all-solid-state battery with the Li/LLTa/$LiCoO_2$ configuration was fabricated by attaching Li metal to the

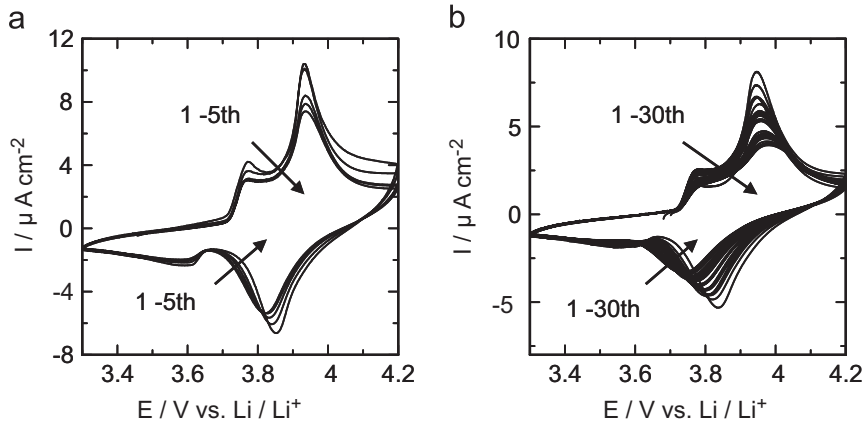

Fig. 9. Cyclic voltammograms of Li/LLTa/$LiCoO_2$ cell (a) just after fabrication and (b) after preservation in an Ar-filled glove box for one year at a scan rate of 1 mV min^{-1}.

LLTa side of the $LiCoO_2$/LLTa pellet. The CV measurements were then conducted on this battery. The resulting cyclic voltammogram is shown in Fig. 9(a). In the anode scan, two distinct oxidation peaks were observed at approximately 3.75 and 3.95 V vs. Li/Li^+, which correspond to the oxidation of LT- and HT-$LiCoO_2$, respectively [28]. There is no doubt that deintercalation of Li ions from the $LiCoO_2$ on the LLTa and the subsequent deposition of Li was occurring during the anode scan. In the cathode scan, reduction peaks were observed as well. It can be concluded that the all-solid-state battery with Li metal anode was successfully created using the LLTa electrolyte. To verify the operation of the battery after long-term storage, CV measurements of the Li/LLTa/$LiCoO_2$ cell were conducted after one year of storage in Ar-filled glove-box (Fig. 9(b)). In the resulting cyclic voltammogram, the redox peaks were distinctively observed, indicating that the cell can be operated successfully even after one year of storage. It can be noted that the interfaces of the $LiCoO_2$/LLTa and LLTa/Li, as well as the LLTa itself, are very stable.

4. Discussion

In this study, the chemical and electrochemical properties of LLTa were examined, and the all-solid-state battery using LLTa electrolyte was fabricated.

The Li ion conductivity of our LLTa pellet was higher than the previously reported value for this material [11]. This can be attributed to the high crystallinity of our LLTa pellet. In this study, a sintering temperature of 1200 °C was selected, whereas the LLTa pellet previously reported was sintered at 950 °C. Indeed, we could not confirm the charge and discharge behaviors in the all-solid-state battery using the LLTa pellet sintered at 900 °C due to the much higher impedance it possessed. The estimated bulk and total Li ion conductivities of the LLTa pellet sintered at 1200 °C were 3.9×10^{-4} and 1.3×10^{-4} S cm^{-1}, respectively, implying that the LLTa pellet is acceptable for use in the all-solid-state lithium battery.

The measurement of the electrochemical window revealed that the LLTa pellet was stable until at least 5 V vs. Li/Li^+. This result implies that high voltage cathode materials, such as $LiCoPO_4$ or $LiNi_{0.5}Mn_{1.5}O_4$, can be utilized in the all-solid-state battery with LLTa solid electrolyte. These cathode materials cannot be utilized in the present lithium battery using liquid electrolytes that include organic solvents because decomposition of the liquid electrolyte is inevitable at high potentials of 5 V vs. Li/Li^+ [29,30]. By using the LLTa solid electrolyte, fabrication of the 5 V class of lithium batteries is possible.

An all-solid-state battery with LLTa solid electrolyte was fabricated by using $LiCoO_2$ cathode and Li metal anode. In the cyclic voltammogram, clear redox peaks were observed at 3.75 and 3.95 V, and these redox peaks corresponded to the redox potentials of the LT- and HT-$LiCoO_2$, respectively. The clear redox peak of LT-$LiCoO_2$ was confirmed in the cyclic voltammogram, although the Raman band of the LT-$LiCoO_2$ (Fig. 9) was barely observed. This LT-$LiCoO_2$ is thought to be formed from the precursor sol for the $LiCoO_2$. To prepare the $LiCoO_2$ cathode, the HT-$LiCoO_2$ powder and the precursor sol for $LiCoO_2$ were mixed and the mixture was impregnated onto the LLTa pellet followed by calcination. The precursor sol is much easier to contact with the LLTa pellet surface due to its fluidity. During the calcination, the precursor sol was converted to LT-$LiCoO_2$. Therefore, LT-$LiCoO_2$ mainly existed on the LLTa surface. Only small amounts of LT-$LiCoO_2$ were formed; however, they could easily participate in the electrochemical reaction due to its proximity to the interface.

It was concluded that the all-solid-state battery with Li metal anode was successfully fabricated. However, the estimated quantities of electricity in the anode and cathode scan at the first cycle of CV were approximately 20 mC. This is only 4% of the calculated value from the theoretical discharge capacity and loading of $LiCoO_2$, assuming that full charge state of the $LiCoO_2$ was $Li_{0.5}CoO_2$. There are two reasons for this low utility of cathode. One is low Li ion and electrical conductivities in the $LiCoO_2$ cathode.

The active material at the current collector side may not be able to participate the battery reaction. To improve the utility of the cathode, the addition of electrically conductive materials, such as Ketjen black, are thought to be useful. The other reason for the low utility of the cathode is thought to be poor contact between the solid electrolyte and the solid $LiCoO_2$ electrode. To obtain better contact, a three dimensional (3D) battery that can provide a large solid–solid contact area is very useful [1,31,32]. We have previously fabricated an all-solid-state 3D battery with 3 dimensionally ordered macroporous (3DOM) structure [9]. A battery composed of $LiMn_2O_4$ cathode and 3DOM LLT solid electrolyte provided quite large discharge capacity, 83 mA h g^{-1}, as the all-solid-state battery. This is 56% of the theoretical capacity [33]. In this 3D configuration, a large amount of active material can be loaded, and the areal capacity can be improved. Accordingly, the fabrication of high performance all-solid-state battery with Li metal anode can be achieved by using 3DOM LLTa solid electrolyte.

The fabrication of the all-solid-state battery using 3DOM LLTa solid electrolyte is under way. New findings will be reported in due course.

5. Conclusions

The chemical and electrochemical properties of $Li_5La_3Ta_2O_{12}$ (LLTa) were investigated to determine its compatibility with an all-solid-state battery with Li metal anode. It was clearly demonstrated that Li ions could move in the LLTa pellet without degradation of the pellet. Additionally, the LLTa electrolyte did not start decomposition until 5 V vs. Li/Li^+. Finally, successful operation of the all-solid-state Li battery with the $Li/LLTa/LiCoO_2$ configuration was achieved, and the battery still worked as a rechargeable battery even after one year of storage in an Ar-filled glove-box. It can be stated that the LLTa solid electrolyte is a promising candidate for the all-solid-state battery because of its relatively high Li ion conductivity, wide electrochemical window, and good stability in contact with Li metal anode and $LiCoO_2$ cathode. To improve the performance of the battery, three dimensional structure is required.

References

[1] M. Kotobuki, Y. Suzuki, H. Munakata, K. Knamaura, Y. Sato, K. Yamamoto, T. Yoshida, Fabrication of three-dimensional battery using ceramics electrolyte with honeycomb structure by sol–gel process, Journal of Electrochemical Society 157 (4) (2010) A493.

[2] M. Kotobuki, K. Kanamura, Y. Sato, K. Yamamoto, T. Yoshida, Electrochemical properties of $Li_7La_3Zr_2O_{12}$ solid electrolyte prepared in argon atmosphere, Journal of Power Sources 199 (2012) 346.

[3] V. Thangadurai, J. Schwenzel, W. Weppner, Tailoring ceramics for specific applications: a case study of the development of all-solid-state lithium batteries, Ionics 11 (2005) 11.

[4] X. Yu, J.B. Bates, G.E. Jellison Jr., F.X. Hart, A stable thin-film lithium electrolyte: lithium phosphorus oxynitride, Journal of the Electrochemical Society 144 (1997) 524.

[5] Y. Inaguma, C. Liquan, M. Itoh, T. Nakamura, T. Uchida, H. Ikuta, M. Wakihara, High ionic conductivity in lithium lanthanum titanate, Solid State Communications 86 (1993) 689.

[6] T. Abe, M. Ohtsuka, F. Sagane, Y. Iriyama, Z. Ogumi, Lithium ion transfer at the interface between lithium-ion-conductive solid crystalline electrolyte and polymer electrolyte batteries, fuel cells, and energy conversion, Journal of the Electrochemical Society 151 (2004) A1950.

[7] H. Aono, E. Sugimoto, Y. Sadaoka, N. Imanaka, G. Adachi, Ionic conductivity of solid electrolytes based on lithium titanium phosphate, Journal of the Electrochemical Society 137 (1990) 1023.

[8] J. Fu, Superionic conductivity of glass–ceramics in the system Li_2O–Al_2O_3–TiO_2–P_2O_5, Solid State Ionics 96 (1997) 195.

[9] M. Hara, H. Nakano, K. Dokko, S. Okuda, A. Kaeriyama, K. Kanamura, Fabrication of all solid-state lithium-ion batteries with three-dimensionally ordered composite electrode consisting of $Li_{0.35}La_{0.55}TiO_3$ and $LiMn_2O_4$, Journal of Power Sources 189 (2009) 485.

[10] P. Knauth, Inorganic solid Li ion conductors: an overview, Solid State Ionics 180 (2009) 911.

[11] V. Thangadurai, H. Kaack, W. Weppner, Novel fast lithium ion conduction in garnet-type $Li_5La_3M_2O_{12}$ (M=Nb, Ta), Journal of the American Ceramic Society 86 (2003) 437.

[12] R. Murugan, V. Thangadurai, W. Weppner, Effect of lithium ion content on the lithium ion conductivity of the garnet-like structure $Li_{5+x}BaLa_2Ta_2O_{11.5+0.5x}$ (x=0–2), Applied Physics A 91 (2008) 615.

[13] V. Thangadurai, W. Weppner, Effect of sintering on the ionic conductivity of garnet-related structure $Li_5La_3Nb_2O_{12}$ and In- and K-doped $Li_5La_3Nb_2O_{12}$, Journal of Solid State Chemistry 179 (2006) 974.

[14] R. Murugan, V. Thangadurai, W. Weppner, Fast lithium ion conduction in garnet-type $Li_7La_3Zr_2O_{12}$, Angewandte Chemie International Edition 46 (2007) 7778.

[15] J.P. Zheng, R.Y. Liang, M. Hendrickson, E.J. Plichta, Theoretical energy density of Li–air batteries and energy storage, Journal of the Electrochemical Society 155 (6) (2008) A432.

[16] H. Fujimoto, A. Mabuchi, K. Tokumitsu, N. Chinnasamy, T. Kasuh, Li nuclear magnetic resonance studies of hard carbon and graphite/hard carbon hybrid anode for Li ion battery, Journal of Power Sources 196 (2011) 1365.

[17] M. Kotobuki, H. Munakata, K. Kanamura, Y. Sato, T. Yoshida, Compatibility of $Li_7La_3Zr_2O_{12}$ solid electrolyte to all-solid-state battery using Li metal anode, Journal of the Electrochemical Society 157 (10) (2010) A1076.

[18] K.H. Kim, Y. Iriyama, K. Yamamoto, S. Kumazaki, T. Asaka, K. Tanabe, C. Fisher, T. Hirayama, R. Murugan, Z. Ogumi, Characterization of the interface between $LiCoO_2$ and $Li_7La_3Zr_2O_{12}$ in an all-solid-state rechargeable lithium battery, Journal of Power Sources 196 (2011) 764.

[19] T.H. Rho, K. Kanamura, T. Umegaki, $LiCoO_2$ and $LiMn_2O_4$ thin-film electrodes for rechargeable lithium batteries, Journal of the Electrochemical Society 150 (2003) A107.

[20] D.R. John, J.T.S. Irvine, D.C. Sinclair, A.R. West, Electroceramics: characterization by impedance spectroscopy, Advanced Materials 2 (1990) 132.

[21] V. Thangadurai, W. Weppner, $Li_6ALa_2Nb_2O_{12}$ (A=Ca, Sr, Ba): a new class of fast lithium ion conductors with garnet-like structure, Journal of the American Ceramic Society 88 (2005) 411.

[22] V. Thangadurai, W. Weppner, $Li_6ALa_2Ta_2O_{12}$ (A=Sr,Ba): novel garnet-like oxides for fast lithium ion conduction, Advanced Functional Materials 15 (2005) 107.

[23] V. Thangadurai, W. Weppner, Investigations on electrical conductivity and chemical compatibility between fast lithium ion conducting garnet-like $Li_6BaLa_2Ta_2O_{12}$ and lithium battery cathodes, Journal of Power Sources 142 (2005) 339.

[24] J. Fu, Y. Bai, C. Liu, H. Yu, Y. Mo, Physical characteristic study of $LiCoO_2$ prepared by molten salt synthesis method in 550–800 °C, Materials Chemistry and Physics 115 (2009) 105.

[25] E. Antolini, $LiCoO_2$: formation, structure, lithium and oxygen nonstoichiometry, electrochemical behaviour and transport properties, Solid State Ionics 170 (2004) 159.
[26] W. Huang, R. Frech, Vibrational spectroscopic and electrochemical studies of the low and high temperature phases of $LiCo_{1-x}$ M_xO_2 (M = Ni or Ti), Solid State Ionics 86–88 (1996) 395.
[27] T. Ohzuku, A. Ueda, Solid-state redox reactions of $LiCoO_2$ ($R\bar{3}m$) for 4 V secondary lithium cells, Journal of the Electrochemical Society 141 (1994) 2972.
[28] E. Rossen, J.N. Reimers, J.R. Dahn, Synthesis and electrochemistry of spinel LT-$LiCoO_2$, Solid State Ionics 62 (1993) 53.
[29] M. Matsui, K. Dokko, K. Kanamura, Surface layer formation and stripping process on $LiMn_2O_4$ and $LiNi_{1/2}Mn_{3/2}O_4$ thin film electrodes, Journal of the Electrochemical Society 157 (2010) A121.
[30] Y. Talyosef, B. Markovsky, G. Salitra, D. Aurbach, H.-J. Kim, S. Choi, The study of $LiNi_{0.5}Mn_{1.5}O_4$ 5 V cathodes for Li-ion batteries, Journal of Power Sources 146 (2005) 664.
[31] M. Kotobuki, Y. Isshiki, H. Munakata, K. Kanamura, All-solid-state lithium battery with a three-dimensionally ordered $Li_{1.5}Al_{0.5}Ti_{1.5}(PO_4)_3$ electrode, Electrochimica Acta 55 (2010) 6892.
[32] M. Kotobuki, Y. Suzuki, H. Munakata, K. Kanamura, Y. Sato, K. Yamamoto, T. Yoshida, Compatibility of $LiCoO_2$ and $LiMn_2O_4$ cathode materials for $Li_{0.55}La_{0.35}TiO_3$ electrolyte to fabricate all-solid-state lithium battery, Journal of Power Sources 195 (2010) 5784.
[33] R.K. Katiyara, R. Singhalb, K. Asmarb, R. Valentina, R.S. Katiyarb, High voltage spinel cathode materials for high energy density and high rate capability Li ion rechargeable batteries, Journal of Power Sources 194 (2009) 526.